STRESS CONCENTRATION AT SLIGHTLY UNDULATING SURFACES

HUAJIAN GAO

Division of Applied Mechanics, Stanford University, Stanford, CA 94305, U.S.A.

(Received 13 February 1990)

ABSTRACT

This paper presents a first-order perturbation analysis of the stress concentration effects caused by slightly undulating surfaces. The perturbation approach that we use treats the undulating surfaces as being perturbed from a reference state in which the surface is perfectly flat. The magnitude of the perturbation is assumed to be sufficiently small compared to other length scales of the bulk material so that a half-plane model can be used for simplification. First-order-accurate perturbation solutions have been derived for the stress distribution along a sinusoidally wavy surface and for the attenuation of the stress concentration away from the undulating surface. The interactions among different surface perturbation waves are investigated by comparing the result of stress concentration factor at the trough of a single wave perturbation along an otherwise flat surface to that for periodically wavy surface. We also examine some of the 3-D effects by using the perturbation algorithm to calculate the stress concentration at undulating surfaces of elastic half-spaces. In all cases, it is found that wavy surfaces can magnify the bulk stress easily by a factor of 2 or 3 when the surface profile does not deviate substantially from flatness. This stress concentration effect is significant especially for already highly stressed heteroepitaxial semiconductor thin films, suggesting that the surface morphology of the film surfaces can play an important role in nucleating dislocations and crack-like surface flaws before the bulk stress reaches a critical level.

Introduction

MECHANICAL failures of structures often result from brittle fracture or plastic deformation nucleated at material surfaces, due to surface defects and inhomogeneities inherited from the manufacturing processes as well as damage from environmental corrosion and impact loadings. In this paper, we examine, via a first-order perturbation algorithm, the stress concentration effects caused by slightly undulating surfaces. The method we use is based on a linear perturbation approach to inclusion and void problems formulated recently by the author (GAO, 1990).

The impetus to undertake the present work also comes from an ongoing effort to understand the surface nucleation of dislocation half-loops in semiconductor heteroepitaxial structures. As reviewed by many authors (e.g. Ploog, 1986; Okamoto, 1987), materials composed of semiconductor layers with different lattice parameters have found numerous applications in electronic and optical devices. The lattice mismatch creates strain which results in formation of dislocations in the structure. The dislocation nucleations are also found in thin film structures that comprise integrated circuit and magnetic disks. It is of extremely high technological importance to reduce

the dislocation densities to manufacture high performance, high yield electronic devices. Nix (1989) recently reviewed some of the mechanical properties of thin films on substrates and pointed out that very large stresses (e.g. 0.5 GPa), generated by strain sources such as thermal mismatch and epitaxial lattice mismatch, may be present to cause plastic deformation and fracture. Under such high stresses, a slight magnification of the bulk stress by surface inhomogeneities such as micro-level bumps and troughs is likely to play a role in triggering nucleation processes of dislocations and cracks.

With the above motivation, we shall investigate the stress concentration at undulating surfaces via a first-order perturbation algorithm. The perturbation approach employs certain known elastic Green's functions for perfectly flat surfaces and treats an undulating surface as being perturbed from a reference flat surface. We carry out the perturbation analysis for sinusoidally wavy surfaces of elastic half-planes, with simple solutions given for the stress concentration factors near the surface. It is found that the slightly wavy surfaces can easily magnify the bulk stress by a factor of 2 or 3 according to

$$S = 1 + 4\pi(A/\lambda) \tag{1}$$

where S is the stress concentration factor, A the wave amplitude and λ the wavelength of the surface. At deeper locations away from the surface, the stress is attenuated exponentially at a characteristic depth about 0.2λ , independent of the wave amplitude A. The perturbation analyses suggest that the surface morphology can sometimes play an important role in nucleating cracks and dislocations before the bulk stress reaches a critical level.

The stress concentration factor at a single wave trough along an otherwise flat surface is also calculated by the linear perturbation approach. The single-wave stress result does not differ much from that for a periodically wavy surface, indicating that the interaction effects among different surface perturbation waves are not substantial. To examine the 3-D effects, we extend the perturbation analysis to slightly undulating surfaces of elastic half-spaces subjected to bi-axial bulk stresses. The 3-D undulating surfaces cause slightly lower, but nevertheless of the same order, stress concentrations compared to their 2-D counterparts.

PERTURBATION APPROACH

In this section we follow a perturbation algorithm formulated earlier in GAO (1990) for elastic inclusion and void problems and present a special version within the context of surface perturbations. The undulating surface of concern here is assumed to be close to a perfectly flat one with perturbation magnitude small compared to other length scales of the bulk material. Hence it suffices to treat an elastic half-plane as we do in the following.

Figure 1 shows a flat surface along the cartesian x-axis. The half-plane is subjected to a uniform lateral bulk stress $\sigma_{xx}^0 = T$, such as the mismatch stresses in semiconductor thin films. In addition to T, a concentrated point force \mathbf{P} is placed at a position (x, y),

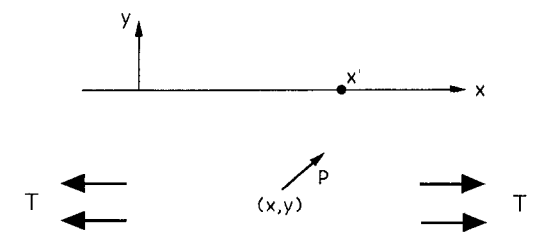


Fig. 1. An elastic half-plane subjected to lateral bulk stress T and a concentrated point force **P** at (x, y).

with $P_i \delta u_i(x, y)$ (subscripts i, j, k, l, \ldots range over x, y) equal to the work done by the force at an incremental displacement $\delta \mathbf{u}(x, y)$.

Imagine that the flat surface is relocated (e.g. by cutting or adding a layer of variable thickness of the same material) to a neighbouring undulating position by some variable normal distance $\delta a(x')$ at a location x' (Fig. 2). Treating $\delta a(x')$ as infinitesimal, the change in total energy Γ (strain energy plus potential energy) of the system is

$$\delta\Gamma = P_i \delta u_i(x, y) + \int_{-\infty}^{\infty} w \delta a(x') \, \mathrm{d}x', \tag{2}$$

where w denotes the strain energy density distribution along the surface. The perturbation term in (2) is consistent with a general energy relation discussed by RICE and DRUCKER (1967).

The energy quantity Γ represents a state variable which can depend only on the magnitude of P_i , u_i and the location of the surface. Therefore the right-hand side of (2) is a perfect differential. Applying a Legendre transformation to (2) and using the Maxwell reciprocal relation, it follows (for details see GAO, 1990) that the variation in the displacement $u_i(x, y)$ associated with the surface perturbation $\delta a(x')$ under the same bulk stress T is

$$\delta u_i(x,y) = -\int_{-\infty}^{\infty} \frac{\partial w}{\partial P_i} \, \delta a(x') \, \mathrm{d}x', \tag{3}$$

where the derivative with respect to P_i is evaluated with the surface held fixed in the original flat position.



Fig. 2. A slightly undulating surface of a half-plane, treated as being perturbed from the reference flat position along the x-axis by $\delta a(x')$.

For linear elastic solids, the strain energy density function w is quadratic in terms of the stress components, i.e.

$$w = \frac{1}{2}\sigma_{ij}\varepsilon_{ij} = \frac{1}{2}S_{ijkl}\sigma_{ij}\sigma_{kl},\tag{4}$$

where S_{ijkl} is the compliance moduli tensor. Along the traction-free surface the strain energy density simplifies to

$$w = \frac{1}{2H} \sigma_{xx}^2, \tag{5}$$

where H = E for plane stress and $H = E/(1-v^2)$ for plane strain; E, v are Young's modulus and Poisson ratio respectively. The relation

$$\frac{\partial w}{\partial P_m} = \sigma_{xx} \Sigma_{xx}^m / H \tag{6}$$

then follows when we identify

$$\Sigma_{xx}^{m}(x'; x, y) = \frac{\partial \sigma_{xx}}{\partial P_{m}} \tag{7}$$

as the surface stress Green's function, i.e. the surface stress at x' due to a unit point force in m direction at x, y.

Equations (3) and (6) must hold no matter what the magnitude of P_i is and in particular, they must hold when $P_i = 0$, corresponding to the original bulk stress condition in absence of the point force P_i . When $P_i = 0$, $\sigma_{xx} = \sigma_{xx}^0 = T$, and (6) yield

$$\delta u_m(x,y) = -\frac{T}{H} \int_{-\infty}^{\infty} \Sigma_{xx}^m(x';x,y) \delta a(x') \, \mathrm{d}x' \tag{8}$$

to first order in $\delta a(x')$. Here $\sum_{xx}^{m}(x'; x, y)$ is the stress Green's function for the elastic half-plane with perfectly flat surface. The displacement variation (8) can be substituted into the constitutive relations to calculate the stress and strain variations due to the perturbation $\delta a(x')$. Of particular interest here is the stress variation

$$\delta\sigma_{ij}(x,y) = -T \int_{-\infty}^{\infty} \hat{\Sigma}_{ij}(x';x,y) \delta a(x') \, \mathrm{d}x'$$
 (9)

where the kernel functions $\hat{\Sigma}_{ij}(x'; x, y)$ may be directly calculated from Green's functions Σ_{xx}^i by

$$\hat{\Sigma}_{ij} = \frac{1}{H} \left[\mu \left(\frac{\partial \Sigma_{xx}^i}{\partial x_i} + \frac{\partial \Sigma_{xx}^j}{\partial x_i} \right) + \frac{2\mu\nu\delta_{ij}}{1 - 2\nu} \frac{\partial \Sigma_{xx}^k}{\partial x_k} \right]$$
(10)

 μ being the shear modulus and δ_{ij} the Kronecker delta. Hence, knowledge of Green's functions $\Sigma_{xx}^m(x'; x, y)$ allows us to calculate, to first order accuracy, the variation of the displacement field by (8) and the variation of the stress field by (9) when the flat surface is perturbed by $\delta a(x')$.

Similar perturbation expressions can be derived for the 3-D geometry of an elastic half-space subjected to bi-axial bulk stresses $\sigma_{xx}^0 = \sigma_{zz}^0 = T$ with surface perturbed

from an initially flat position in the x, z plane to a slightly undulating position by a variable normal distance $\delta a(x', z')$. In that case, one can show, similarly to (8), that

$$\delta u_m(x,y,z) = -\frac{(1-v)T}{E} \int_{-\infty}^{\infty} \int_{-\infty}^{\infty} \Sigma^m(x',z';x,y,z) \delta a(x',z') \,\mathrm{d}x' \,\mathrm{d}z' \qquad (11)$$

where

$$\Sigma^{m}(x', z'; x, y, z) = \Sigma_{xx}^{m}(x', z'; x, y, z) + \Sigma_{z}^{m}(x', z'; x, y, z).$$
 (12)

Here $\Sigma_{xx}^m(x',z';x,y,z)$, $\Sigma_{zz}^m(x',z';x,y,z)$ are the 3-D stress Green's functions for elastic half-spaces, e.g. $\Sigma_{xx}^m(x',z';x,y,z)$ is the stress component σ_{xx} at surface location x',z' due to a unit point force in m direction at x,y,z. Subscripts i,j,k,l range over x,y,z in the 3-D regime. The 3-D Green's functions Σ^m for an elastic half-space may be extracted from the point force solutions of MINDLIN (1936). Analogously to (9), one can also write the stress variation in three dimension as

$$\delta\sigma_{ij}(x,y,z) = -T \int_{-\infty}^{\infty} \int_{-\infty}^{\infty} \hat{\Sigma}_{ij}(x',z';x,y,z) \delta a(x',z') \, \mathrm{d}x' \, \mathrm{d}z'. \tag{13}$$

The 3-D stress kernel functions $\hat{\Sigma}_{ij}(x',z';x,y,z)$ are determined from the Green's functions Σ^m in a similar fashion to (10).

Based on (8) and (9), a first-order perturbation approach to undulating surfaces is formulated as follows. Assume the magnitude of the surface undulation is sufficiently small. Then the given surface profile may be viewed as being perturbed from a *reference* flat surface by a small perturbation $\delta a(x')$. The displacements and stresses for the undulating surface are then written as

$$u_i(x, y) = u_i^0(x, y) + \delta u_i(x, y), \quad \sigma_{ii}(x, y) = \sigma_{ii}^0(x, y) + \delta \sigma_{ii}(x, y),$$
 (14)

where $u_i^0(x, y)$, $\sigma_{ij}^0(x, y)$ are the displacements and stresses in the reference state, i.e. the half-plane with a perfectly flat surface under lateral bulk stress T, and $\delta u_i(x, y)$, $\delta \sigma_{ij}(x, y)$ are those given in (8), (9). The 3-D perturbation formulae (11), (13) provide an extension to surfaces undulating in both x and z dimensions.

STRESS CONCENTRATION AT UNDULATING SURFACES: 2-D CASES

The crucial quantities in carrying out the perturbation analysis are the stress Green's functions Σ_{ij}^m which may be extracted from the following point force solutions for a half-plane quoted from Green and Zerna (1968). When a point force **P** acts at a position z = x + iy (Fig. 1), the surface stress can be written as

$$\sigma_{xx}(x'; x, y) = 4 \operatorname{Re} \left[\Omega(x', z)\right] \tag{15}$$

where the complex potential $\Omega(x'; z)$ is given by

$$\Omega(x';z) = -\frac{Q}{x'-z} + \frac{\bar{Q}(z-\bar{z})}{(x'-\bar{z})^2} - \frac{\kappa Q}{x'-z}, \quad Q = \frac{P_x + iP_y}{2\pi(\kappa+1)}.$$
 (16)

Here $\kappa = 3 - 4\nu$ for plane strain and $\kappa = (3 - \nu)/(1 + \nu)$ for plane stress. The stress

Green's functions Σ_{xx}^m are extracted from the above elasticity solutions by alternating $(P_x, P_y) = (1,0)$, (0,1), which in turn leads to the derivation of the stress kernel functions $\hat{\Sigma}_{ij}$. Without presenting the lengthy but straightforward algebraic manipulations we find

$$\hat{\Sigma}_{xx}(x';x,y) = -\frac{2}{\pi} \operatorname{Re} \left[\frac{x'-x}{(x'-z)^3} \right], \quad \hat{\Sigma}_{yy}(x';x,y) = -\frac{2}{\pi} \operatorname{Im} \left[\frac{y}{(x'-z)^3} \right],$$

$$\hat{\Sigma}_{xy}(x';x,y) = \frac{2}{\pi} \operatorname{Re} \left[\frac{y}{(x'-z)^3} \right]. \tag{17}$$

These stress kernel functions, when substituted into (9), give the stress variations due to arbitrary surface perturbation $\delta a(x')$. Along the surface plane y = 0,

$$\hat{\Sigma}_{xx}(x',x) = -\frac{2}{\pi(x'-x)^2},\tag{18}$$

so that the stress σ_{xx} has been increased from the bulk stress level T to

$$\sigma_{xx}(x) = T \left[1 + \frac{2}{\pi} \int_{-\infty}^{\infty} \frac{\delta a(x')}{(x'-x)^2} \, \mathrm{d}x' \right]. \tag{19}$$

Within first-order accuracy, the tangential stress component at the undulating surface is equal to σ_{xx} as given in (19), although the tangent has been perturbed slightly from the x direction.

Curiously, (19) is similar in form to a formula given by RICE (1985) for the variation of stress intensity factor at a half-plane crack front when the front is perturbed to a neighbouring position. As RICE (1985) pointed out in his work within the context of crack perturbation, the kind of singular integral expressed in (19) has a principal value in the Cauchy sense only when the perturbation $\delta a(x')$ satisfies

$$\delta a(x) = 0 \tag{20}$$

at the observation point x since otherwise the stress kernel function has an inadmissible singularity at x' = x. Fortunately, one has the freedom to relocate the reference flat surface so that the condition (20) can always be met, because the reference state is merely a virtual concept in the perturbation scheme. Under the bulk stress T the Green's function solutions Σ_{xx}^m for the reference flat surface are independent of the vertical location of the reference surface with respect to the wavy surface. This indicates that one may freely relocate the reference surface plane without affecting the form of stress kernel functions $\hat{\Sigma}_{ij}$ expressed in (17), (18) if the variables x-x', y are understood in the relative sense as the horizontal and vertical distances from the observation point (x, y) to the perturbation point (x') along the reference surface.

A simple treatment of the inadmissible singularity in (19) is given as follows. Assume that the given undulating surface can be described by the function a(x') which measures the distance from the x-axis to the surface at a position x'. At the chosen

observation point x, we shall relocate the reference surface along a straight line at a distance a(x) to the x-axis so that

$$\delta a(x') = a(x') - a(x) \tag{21}$$

vanishes at x' = x. Therefore by (19, 21) we may write the rigorously valid perturbation formula as

$$\sigma_{xx}(x) = T \left[1 + \frac{2}{\pi} PV \int_{-\infty}^{\infty} \frac{a(x') - a(x)}{(x' - x)^2} dx' \right], \tag{22}$$

accurate to first order in a(x') - a(x) for arbitrary surface profile a(x') that differs slightly from constancy. Here PV denotes principal value in the Cauchy sense.

For comparison, RICE's (1985) formula for the variation of stress intensity factor along a slightly curved crack front described by y = c(x) can be written in our notation as

$$K(x) = K^{0} \left[1 + \frac{1}{2\pi} PV \int_{-\infty}^{\infty} \frac{c(x') - c(x)}{(x' - x)^{2}} dx' \right], \tag{23}$$

where K^0 is the stress intensity factor along a perfectly straight crack front. The analogy between the surface perturbation and the crack perturbation has been pointed out earlier by GAO (1990). Using an integration by parts, one can also recast (22) into a familiar form of Cauchy-type integral equation

$$\frac{\sigma_n(x) - T}{T} = \frac{2}{\pi} PV \int_{-\infty}^{\infty} \frac{\mathrm{d}a(x')/\mathrm{d}x'}{x' - x} \,\mathrm{d}x' \tag{24}$$

which establishes an analogy between the present problem for surface perturbations to various others such as representing cracks by continuous arrays of dislocations, Hertzian contact mechanics of a rigid punch on a half-plane, elastic-plastic plane stress Dugdale crack model, etc.

The stress attenuation away from the surface is to be calculated by substituting the kernel functions of (17) into (9), replacing y by y-a(x) and $\delta a(x')$ by a(x')-a(x). Hence,

$$\sigma_{xx}(x,y) = T \left\{ 1 + \frac{2}{\pi} \int_{-\infty}^{\infty} \text{Re} \left[\frac{x' - x}{(x' - x - i[y - a(x)])^3} \right] [a(x') - a(x)] \, dx' \right\},$$

$$\sigma_{yy}(x,y) = \frac{2T}{\pi} \int_{-\infty}^{\infty} \text{Im} \left[\frac{y - a(x)}{(x' - x - i[y - a(x)])^3} \right] [a(x') - a(x)] \, dx',$$

$$\sigma_{xy}(x,y) = -\frac{2T}{\pi} \int_{-\infty}^{\infty} \text{Re} \left[\frac{y - a(x)}{(x' - x - i[y - a(x)])^3} \right] [a(x') - a(x)] \, dx',$$
(25)

where |y-a(x)| is the vertical distance from the observation point (x,y) to the reference flat surface y=a(x).

As applications two simple cases of undulating surfaces are studied in the following.

Sinusoidally wavy surface

Consider a sinusoidally wavy surface whose shape is described by the cosine wave function

$$a(x) = a_0 - A\cos(2\pi x/\lambda). \tag{26}$$

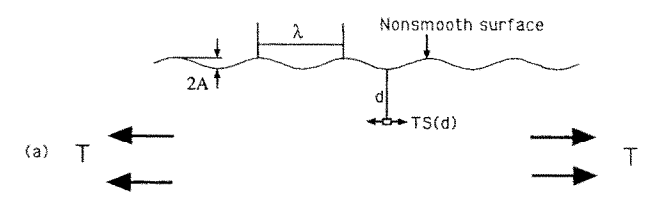
As shown in Fig. 3(a), (26) describes a wavy surface with wave amplitude A > 0 and wavelength λ . The constant a_0 can be arbitrary which is irrelevant to our final perturbation results. For first-order perturbations the wave amplitude A is assumed to be small so that $A/\lambda \ll 1$. Using (22), (26), the stress distribution along the wavy surface of (26) is found to be

$$\sigma_{xx}(x) = T[1 + 4\pi(A/\lambda)\cos(2\pi x/\lambda)]. \tag{27}$$

The maximum stress concentration factor

$$S = \sigma_{xx}(n\lambda)/T = 1 + 4\pi(A/\lambda) \quad (n = \text{integer})$$
 (28)

occurs when $\cos(2\pi x/\lambda) = 1$, corresponding to the most concave surface locations



Stress concentration factor:

 $S(d)=1+4\pi(A/\lambda)$ $(1-\pi d/\lambda) \exp(-2\pi d/\lambda)$

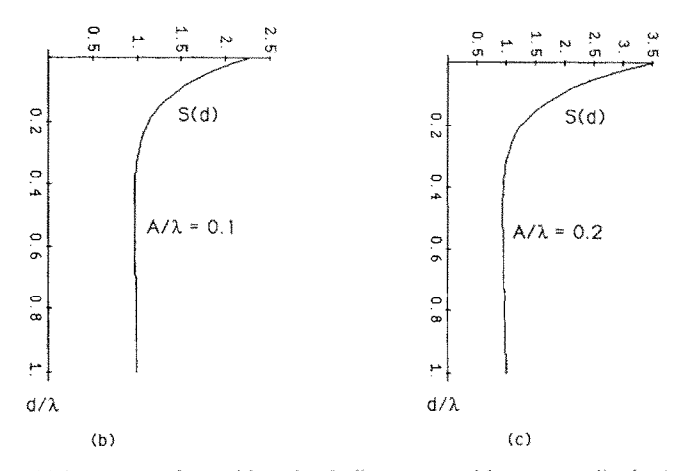


Fig. 3. (a) A sinusoidally wavy surface subjected to bulk stress T, with wave amplitude A and wavelength λ . The stress concentration at a depth d from the surface for (b) $A/\lambda = 0.1$ and (c) $A/\lambda = 0.2$.

(wave troughs) $x = n\lambda$ $(n = 0, \pm 1,...)$. At the most convex location (wave peaks) $x = (2n+1)\lambda/2$ the stress has been reduced from the bulk stress level T due to the shielding effect of the wave troughs.

The remarkable fact is: the magnitude of the stress concentration depends on the ratio A/λ of the wavy surface with a constant coefficient equal to $4\pi = 12.566$, suggesting that slight perturbations can magnify the bulk stress T easily by a factor of 2 or 3. For example, according to perturbation theory, an undulating surface with $A/\lambda = 0.1$ can magnify the bulk stress by 2.25 times.

The stress attenuation away from the surface can be calculated from (25). At a depth d from the surface, we have y-a(x)=d so that the stress component $\sigma_{xx}(x,d)$ is determined by the first of (25) as

$$\sigma_{xx}(x,d)/T = 1 + \frac{2A}{\pi} \left[\int_{-\infty}^{\infty} \frac{t^2(t^2 - 3d^2)}{(t^2 + d^2)^3} \left(1 - \cos \frac{2\pi t}{\lambda} \right) dt \right] \cos \frac{2\pi x}{\lambda}.$$
 (29)

The integral part within the square bracket in (29) can be written as the real part of

$$\int_{-\infty}^{\infty} \frac{t^2(t^2-3d^2)}{(t^2+d^2)^3} (1-e^{2i\pi t/\lambda}) dt.$$

Treating the above as part of the integration along the closed contour enclosing the upper half of the complex t plane, one can evaluate the integral by employing Cauchy's residue theorem. In the upper half t plane, the only singularity of the integrand is a third-order pole at t = di. Evaluating the residue of the integrand at t = di, one can simplify (29) to closed-form solution. Following similar steps for $\sigma_{yy}(x, d)$ and $\sigma_{xy}(x, d)$, one finally has

$$\sigma_{xx}(x,d) = T \left[1 + \frac{4\pi A}{\lambda} \left(1 - \frac{\pi d}{\lambda} \right) e^{-2\pi d/\lambda} \cos \frac{2\pi x}{\lambda} \right],$$

$$\sigma_{yy}(x,d) = \frac{4\pi^2 dAT}{\lambda^2} e^{-2\pi d/\lambda} \cos \frac{2\pi x}{\lambda},$$

$$\sigma_{xy}(x,d) = \frac{2\pi AT}{\lambda} \left(1 - \frac{2\pi d}{\lambda} \right) e^{-2\pi d/\lambda} \sin \frac{2\pi x}{\lambda}.$$
(30)

Thus, in deeper locations away from the surface the stress is attenuated with the characteristic depth $\lambda/2\pi$, independent of the wave amplitude A. At the wave trough locations x = d = 0, (30) recovers the maximum surface stress concentration factor of (28). For graphical description, the attenuation profile of the stress concentration $S(d) = \sigma_{xx}(0, d)/T$, corresponding to the depth attenuation from the wave trough locations, is plotted in Fig. 3(b,c) for $A/\lambda = 0.1, 0.2$.

The perturbation solutions (30), for sinusoidally wavy surfaces, are consistent with those derived recently by SROLOVITZ (1989) who followed a different approach via Airy stress functions.

Single wave perturbation on a flat surface

Interpretation of the perturbation results suggests that a thin layer exists beneath undulating surfaces where the stress concentration is sensitive to the actual surface

morphology. In real situations the surface profiles will be complicated compared to the sinusoidal wavy shapes we have discussed. Still, there is one aspect we may examine by simple analysis, that is, the interaction effects among different surface bumps and troughs. For this purpose we consider the case of one single perturbation wave on an otherwise perfectly flat surface as shown in Fig. 4, in which case there is no interaction with other perturbation waves.

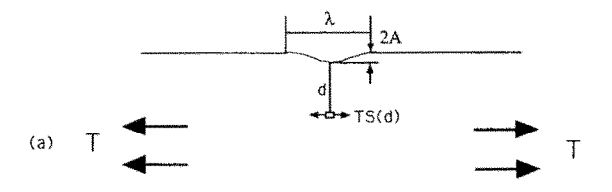
Figure 4(a) depicts the single wave perturbation on an otherwise perfectly flat surface. The surface profile can be written as

$$a(x) = \begin{cases} a_0 + A & |x| \ge \lambda/2\\ a_0 - A\cos(2\pi x/\lambda) & |x| \le \lambda/2. \end{cases}$$
(31)

Substituting (31) into (22), it can be shown that the surface stress reaches the maximum at the wave trough x = 0 with the stress concentration factor

$$S = 1 + 14.813(A/\lambda). \tag{32}$$

In the present case without any interaction effects among different surface waves, the



Maximum stress concentration factor:

$$S(0)=1+14.813(A/\lambda)$$

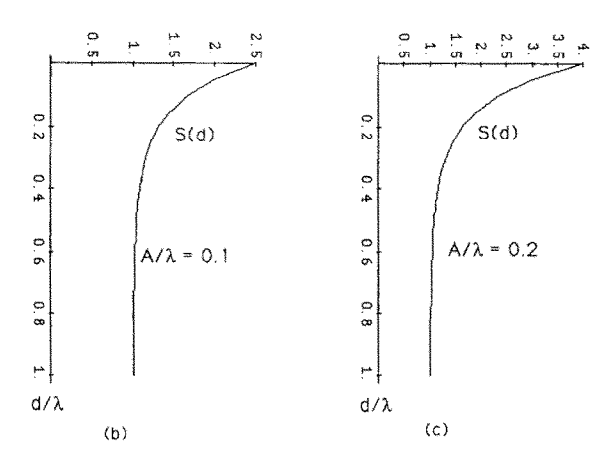


Fig. 4. (a) A single wave trough on an otherwise flat surface subjected to bulk stress T, with perturbation magnitude 2A and length λ . The stress concentration at a depth d from the wave trough for (b) $A/\lambda = 0.1$ and (c) $A/\lambda = 0.2$.

value 14.813 of stress coefficient has increased by 20% over the periodically wavy surface value of 12.566 derived previously (28). This indicates that interactions among different surface waves relax slightly, but not substantially, the stress concentration.

Figure 4(b, c) contains plots of the depthwise stress attenuation profiles for $A/\lambda = 0.1$ and $A/\lambda = 0.2$. The stress attenuation profiles appear to be completely similar to the periodical wave cases shown in Fig. 3. Both cases show characteristic attenuation depth approximately equal to 0.2λ .

As discussed in the Introduction, for heteroepitaxial semiconductor thin film structures, it is not uncommon to find bulk stress T as high as 0.5 GPa due to thermal or lattice mismatches. Assume that the surface morphology of the films displays slight undulations at the microlevel with $A/\lambda=0.1$. Our perturbation results then suggest that the surface stress may be magnified to a level around 1 GPa, much higher than the bulk stress value. Therefore, at least in the highly stressed thin films, the surface morphology can play an important role in activating formations of dislocations and cracks. Once formed, these surface flaws can cause significant strength degradation and malfunction of semiconductor devices, sometimes even leading to ultimate structural failure before the bulk stress reaches a critical level.

STRESS CONCENTRATION AT 3-D UNDULATING SURFACES

The perturbation analysis has been carried out in 2-D configurations. One also wonders how large are the effects that more realistic 3-D undulating surfaces may have on the stress concentrations. To examine some of the 3-D effects, we extend the perturbation analysis to surfaces of elastic half-spaces shown in Figs 5 and 6.

To proceed we need to calculate the Green's functions for an elastic half-space. The elasticity problem of a half-space subjected to a concentrated point force has been solved over half a century ago by MINDLIN (1936). When a unit point force is placed at position (0,0,c), the elastic displacements can be determined through Papkovitch—Neuber potential representation (Papkovitch, 1932)

$$\mathbf{u} = \mathbf{B} - \frac{1}{4(1-\nu)} \nabla (\mathbf{x} \cdot \mathbf{B} + \beta), \tag{33}$$

where B_i (i = x, y, z) and β are the 3-D potential functions. If the point force is normal to the surface y = 0, Mindlin (1936) showed that $B_x = B_z = 0$ and

$$B_{y} = \frac{1}{4\pi\mu} \left[\frac{1}{R_{1}} + \frac{3-4\nu}{R_{2}} + \frac{2c(y+c)}{R_{2}^{3}} \right],$$

$$\beta = \frac{1}{4\pi\mu} \left[4(1-\nu)(1-2\nu)\log(R_{2}+y+c) - \frac{c}{R_{1}} - \frac{c(3-4\nu)}{R_{2}} \right],$$
(34)

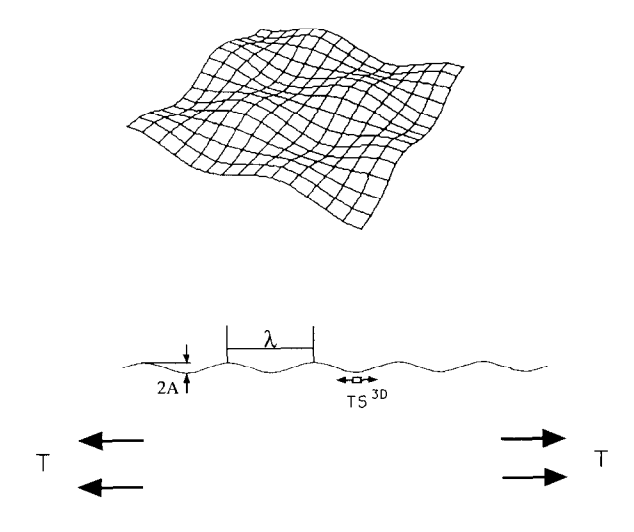
where

$$R_1 = \sqrt{x^2 + (y - c)^2 + z^2}, \quad R_2 = \sqrt{x^2 + (y + c)^2 + z^2}.$$
 (35)

If the point force is parallel to the surface in the x-direction, then we have $B_z = 0$ and

454 H. GAO

3D Surface of a half-space:



Stress Concentration Factor

$$S^{3D} = 1 + 8.89 (1 + v) A/\lambda$$

Fig. 5. A 3-D sinusoidally wavy surface of an elastic half-space subjected to bi-axial bulk stress T; the wave amplitude A and wavelength λ .

$$B_{x} = \frac{1}{4\pi\mu} \left(\frac{1}{R_{1}} + \frac{1}{R_{2}} \right), \quad B_{y} = \frac{1}{2\pi\mu} \left[\frac{(1-2\nu)x}{R_{2}(R_{2}+y+c)} - \frac{cx}{R_{2}^{3}} \right],$$

$$\beta = \frac{1}{2\pi\mu} \frac{(1-2\nu)}{R_{2}+y+c} \left[-(1-2\nu)x + \frac{cx}{R_{2}} \right]. \tag{36}$$

By symmetry the corresponding solutions for a point force in the z-direction are exactly those of (36) if x is replaced by z.

The stress Green's functions Σ^m and the kernel functions $\hat{\Sigma}_{kl}$ can be constructed from the Mindlin solutions given above. To simplify the algebraic manipulations, we only derive the stress kernel functions for surface locations y = 0 where the maximum stress concentration effect occurs. After lengthy algebra we find $\Sigma^y = \hat{\Sigma}_{yy} = 0$,

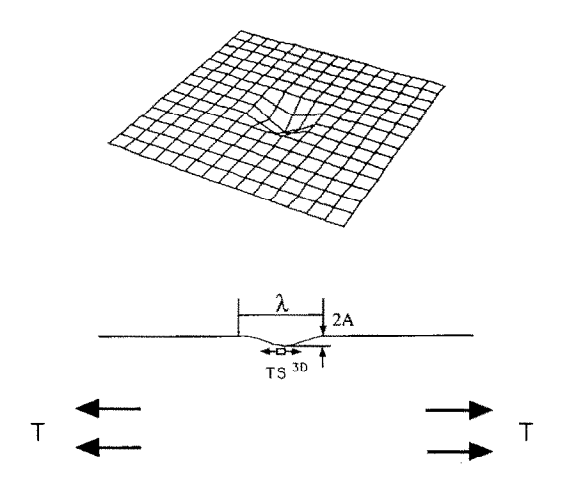
$$\Sigma^{x} = -\frac{(1+v)(x'-x)}{\pi r^{3}}, \quad \Sigma^{z} = -\frac{(1+v)(z'-z)}{\pi r^{3}},$$

where

$$r = \sqrt{(x - x')^2 + (z' - z)^2}$$
 (37)

and

3D Surface of a half-space:



Stress Concentration Factor:

$$S^{3D} = 1 + 14.55 \text{ A}/\lambda$$

Fig. 6. A single wave trough on an otherwise flat surface of an elastic half-space subjected to bi-axial bulk stress T; the perturbation magnitude 2A and length λ .

$$\hat{\Sigma}_{xx}(x',z';x,z) = \frac{-(2-\nu)(x'-x)^2 + (1-2\nu)(z'-z)^2}{\pi r^5},$$

$$\hat{\Sigma}_{zz}(x',z';x,z) = \frac{-(2-\nu)(z'-z)^2 + (1-2\nu)(x'-x)^2}{\pi r^5}.$$
(38)

Along an undulating surface whose shape is described by y = a(x', z'), the surface stress concentration is given by

$$\frac{\sigma_{xx}}{T} = 1 + \int_{-\infty}^{\infty} \int_{-\infty}^{\infty} \frac{(2-\nu)(x'-x)^2 - (1-2\nu)(z'-z)^2}{\pi r^5} [a(x',z') - a(x,z)] \, \mathrm{d}x' \, \mathrm{d}z',$$
(39)

where we have chosen a reference flat surface, similar to the 2-D cases discussed before, at a distance a(x, z) to the x, z plane so that the singular integral of (39) can be defined rigorously in the principal value sense. If a(x, z) is independent of z, one may verify that (39) reduces to the corresponding 2-D formula (22). The stress component $\sigma_{zz}(x, z)$ can be written in a similar form.

We apply the perturbation formula (39) to a sinusoidally wavy surface and a flat surface with a single wave perturbation shown in Figs 5 and 6.

Sinusoidally wavy surface

We consider the sinusoidally wavy surface

$$a(x, z) = a_0 - A\cos(2\pi x/\lambda)\cos(2\pi z/\lambda) \tag{40}$$

as shown in Fig. 5, where A, λ are the wave amplitude and wavelength of the surface. The maximum stress concentration occurs at the most concave locations, i.e. the wave troughs such as x = z = 0 where we find the maximum stress concentration factor $S^{3D} = \sigma_{xx}(0,0)/T$ equal to

$$S^{3D} = 1 + \frac{A}{\pi} \int_{-\infty}^{\infty} \int_{-\infty}^{\infty} \frac{(2 - v)x^2 - (1 - 2v)z^2}{(x^2 + z^2)^{5/2}} \left[1 - \cos\left(\frac{2\pi x}{\lambda}\right) \cos\left(\frac{2\pi z}{\lambda}\right) \right] dx dz$$
$$= 1 + 2\sqrt{2}(1 + v)\pi(A/\lambda). \tag{41}$$

Comparing S^{3D} to the corresponding 2-D value S expressed in (28), one observes that the stress concentration can be slightly relaxed, for Poisson ratio $0 < v < \sqrt{2-1}$, by allowing perturbations along the z-direction. This is not unexpected since we have seen that the interaction among perturbation waves results in relaxation of stress concentration. The 2-D configurations have restricted the surface undulation to along the x-direction, hence may cause higher stress than the more realistic 3-D configuration. For most of the materials, the Poisson ratio v ranges from 0.25 to 0.35, which corresponds to 3-D relaxation by 5% to 12%. Interestingly enough, near the incompressible limit when $\sqrt{2-1} < v < 0.5$, the 3-D undulation actually increases the stress concentration by up to 6%.

Single wave perturbation

Parallel to the 2-D analyses, we also consider a single wave perturbation on an otherwise flat surface as shown in Fig. 6. For simplicity consider the symmetric surface profile

$$a(r) = \begin{cases} a_0 + A & r \geqslant \hat{\lambda}/2\\ a_0 - A\cos(2\pi r/\hat{\lambda}) & r \leqslant \hat{\lambda}/2, \end{cases}$$
(42)

where $r = \sqrt{x^2 + z^2}$. The surface stress attains the maximum at the trough location r = 0. Substituting (42) into (39), we find that, for v = 0.25,

$$S^{3D} = 1 + 14.5451(A/\lambda). \tag{43}$$

The stress coefficient value 14.5451 is close to the corresponding 2-D value 14.813 with approximately 2% difference, showing that the 3-D effects are negligible in the case of a single perturbation wave.

DISCUSSION

We have presented in this paper a first-order perturbation analysis of the stress concentrations along undulating surfaces. The perturbation algorithm follows a recent development of a perturbation approach to elastic inclusion and void problems by GAO (1990). The undulating surfaces are viewed as being perturbed from a reference state in which the surface is perfectly flat. Perturbation solutions are given for the stress concentrations along sinusoidally wavy surfaces and surfaces with a single wave trough. It is found that even slightly undulating surfaces can magnify the bulk stress easily by a factor of 2 or 3. Away from the surface the stress concentration effect is attenuated exponentially at a characteristic depth about one-fifth of the undulating wavelength. Mechanical properties of structures with high bulk stresses such as semiconductor films are likely to be sensitive to surface morphology. With the stress concentration near the surface, damaging surface cracks and dislocations may be nucleated before the bulk stress reaches a critical level. The 3-D effects of undulating surfaces are studied by examining the perturbations of elastic half-spaces using Mindlin's Green function solutions. The largest stress concentration is found for the case of a single surface trough on an otherwise flat surface. This effect drops at increasing interactions among different surface bumps and troughs. The smallest stress concentration effect occurs for surfaces with maximum numbers of perturbation waves.

One may question the range of validity of the first-order perturbation analysis, i.e. whether it is proper at all for the present surface perturbation problem. Of course, the present perturbation analysis could be subjected to verification by exact calculations such as the numerical analyses by finite elements or boundary elements. Nevertheless, we can gain some confidence from a number of previous works cited in the following. First, the linear perturbation analysis for surface perturbations follows the perturbation algorithm formulated by GAO (1990) for general inclusion and void problems. Gao (1990) has examined the range of validity of the perturbation algorithm by using it to compute the stress concentration at an elliptical hole. It was found that the first-order-accurate perturbation results are within 5% of the exact solution when the aspect ratio of the ellipse is as large as 1.6 and within 10% when the aspect ratio is as large as 2. Hence at least in that case, the perturbation analysis can be applied to substantially large magnitude of perturbations. Second, the perturbation analysis for inclusion, void and surface perturbation problems has close analogy to the firstorder crack perturbation theory which was formulated by RICE (1985) and further developed by GAO and RICE (1987, 1989). The previous experiences with crack perturbation analyses indicate that the linear perturbation results are valid for a broad range of perturbation magnitude. For example, GAO and RICE (1987) have applied the crack perturbation analysis to calculate the stress intensity factor along an elliptical crack front and found that the perturbation results match the corresponding exact solution fror aspect ratios as large as 2, similar to the validity range for the perturbation analysis of an elliptical hole (GAO, 1990). Also, GAO and RICE (1989) compared the linear perturbation results for a half-plane crack to the numerical results of FARES (1989) obtained through boundary element (BEM) computations and found that the perturbation results are within 7% of the BEM results when the ratio A/λ (wave 458 H. GAO

amplitude over wavelength) is as large as 0.1. All these suggest that the present surface perturbation results are valid at least for A/λ of order 0.1.

ACKNOWLEDGEMENTS

The work reported was supported by the NSF Research Initiation Award and the NSF-MRL program through the Center for Material Research at Stanford University. The author is extremely grateful for the discussions with Professor W. D. Nix and Professor E. Arzt.

REFERENCES

	1000	* 1 14 1 #4 00#
Fares, N.	1989	J. appl. Mech. 56, 837.
GAO, H.	1990	J. appl. Mech., in review.
GAO, H. and RICE, J. R.	1987	Int. J. Fracture 33, 155.
GAO, H. and RICE, J. R.	1989	J. appl. Mech. 56 , 828.
GREEN, A. E. and ZERNA, W.	1968	Theoretical Elasticity, 2nd Edn. Oxford University
		Press, London.
MINDLIN, R. D.	1936	Physics 7, 195.
Nix, W. D.	1989	Institute of Metals Lecture, Stanford, CA.
Окамото, Н.	1987	Jap. J. appl. Phys. 26 , 315.
PAPKOVITCH, P. F.	1932	Computes Rendus, Acad. des Sciences, Paris, 195,
		513.
Ploog, K.	1986	J. Crystal Growth 79, 887.
RICE, J. R.	1985	J. appl. Mech. 52 , 571
RICE, J. R. and DRUCKER, D. C.	1967	Int. J. Fracture Mech. 3, 19.
Rongved, L.	1955	In Proc. 2nd Midwestern Conf. on Solid Mech.
		(edited by J. L. BODGANOFF), pp. 1-13.
		Edwards Bros., Ann Arbor, MI.
Srolovitz, D. J.	1989	Acta Metall. 37, 621.